Dynamics of ventilated coherent cold eddies on a sloping bottom

By GORDON E. SWATERS[1] AND GLENN R. FLIERL[2]

[1] Applied Mathematics Institute, Department of Mathematics *and* Institute of Earth and Planetary Physics, University of Alberta, Edmonton, Alberta, T6G 2G1, Canada

[2] Center for Meteorology and Physical Oceanography, Department of Earth, Atmospheric and Planetary Sciences, Massachusetts Institute of Technology, Cambridge, MA 02139, USA

A theory is presented to describe the propagation and structure of coherent cold-core (mesoscale) eddies on a sloping bottom including dynamical and thermodynamical interaction with the surrounding fluid. Based on parameter values suggested by oceanographic and rotating-tank experimental data, the evolution of the baroclinic eddy is modelled with nonlinear 'intermediate lengthscale' geostrophic dynamics which is coupled to the surrounding fluid. The process of ventilation is modelled with a simple cross-interfacial mass flux parameterization. The surrounding fluid is governed by nonlinear quasi-geostrophic dynamics including eddy-induced vortex-tube compression. Assuming a relatively weak ventilation rate, a multiple-scale asymptotic theory is constructed to describe the propagation of an initially isolated or coherent baroclinic eddy. Throughout the evolution the eddy is assumed to be interacting strongly with the surrounding fluid. To leading order, the eddy and surrounding fluid satisfy the Stern isolation constraint. The magnitude of the Eulerian velocity field in the surrounding fluid above the eddy is shown to be larger than the swirl velocities in the eddy interior as suggested by experimental data. Also, to leading order, the along-shelf translation speed is given by the Nof formula. The process of ventilation is shown to induce a slowly decaying upslope translation in the propagating eddy, and acts to stimulate a weak slowly decaying topographic Rossby wave field in the surrounding fluid. The important features of the theory are illustrated with a simple example calculation.

1. Introduction

Interesting mesoscale oceanographic features that are found in the continental shelf regions of the world oceans are propagating bottom-trapped coherent cold domes or pools (e.g. Ou & Houghton 1982; Houghton *et al.* 1982; Armi & D'Asaro 1980, among many others). It is thought that these oceanographic features may play a significant role in the mesoscale dynamics of benthic boundary layers on continental shelves and may provide a mechanism for along-shelf nutrient mixing etc. Similar bottom-trapped isolated eddies have also been reproduced experimentally in rotating tanks (e.g. Mory 1983; Mory, Stern & Griffiths 1987; Whitehead *et al.* 1989). As well, there have been some theoretical studies on the dynamics of cold-core eddies (e.g. Nof 1983, 1985; Mory 1985; Mory *et al.* 1987; see also Whitehead *et al.* 1990).

However, these studies, notwithstanding their importance, have been mainly focused on determining the *translation* speed of the eddy or on determining the

general integral constraints that these eddies must satisfy. There has as yet been no complete analysis on the detailed internal structure and interaction characteristics of these eddies with the surrounding fluid. The principal purpose of this paper is to present a unified asymptotic theory describing the propagation and structure of coherent cold-core domes on a sloping bottom and their (dynamical and thermodynamical) interaction with the surrounding fluid.

One important conclusion of the analysis presented by the Nof (1983) study was that, in the absence of any interaction of the eddy with the surrounding environment, the along-shelf propagation speed was given simply by $g's^*/f_0$ (hereafter called the *Nof speed*), where g', s^* and f_0 are the reduced gravity, the constant topographic slope and the Coriolis parameter, respectively, and that the transverse or cross-shelf velocity was identically zero. Note that the Nof speed is independent of the detailed spatial structure of the eddy and depends only on the density difference between the eddy and the surrounding fluid, the bottom slope and the constant Coriolis parameter. The order of magnitude of the along-shelf speed predicted by the Nof formula is in qualitative agreement with the observations presented by Houghton *et al.* (1982). However, the data taken from the rotating-tank experiments described by Mory *et al.* (1987) did not completely agree with the Nof theory. The experiments clearly indicated that a non-negligible cross-shelf drift was present. Another interesting observation was that the azimuthal velocity field above the eddy in the surrounding water was appreciable and was probably larger in magnitude than the swirl velocity in the eddy interior. This last observation strongly suggests that it is important to include the dynamical response of the surrounding fluid in determining the evolution of an initially isolated cold-core eddy.

Mory *et al.* (1987) suggested various mechanisms which may account for the above discrepancies. The first proposal centred on the action of an induced wave drag on the dome due to the excitation of topographic vorticity waves generated by the baroclinic vortex-tube compression associated with the passage of the cold dome through the surrounding fluid. Earlier work by Flierl (1984a) had shown how this drag could result in a mean meridional drift for surface trapped warm eddies on a β-plane.

A second mechanism suggested by Mory *et al.* (1987) was that frictional forces between the eddy and the bottom (which in the experimental configuration may have been particularly important) could result in cross-shelf motion. Mory *et al.* (1987) were unable, however, to distinguish which of these two mechanisms was dynamically dominant in their experiment.

A third effect that may have dynamical importance, especially in the oceanographic context, is the process of ventilation between the cold eddy and the surrounding relatively warmer slope water. Ou & Houghton (1982) argued that this effect was of particular importance during the evolution of the cold dome observed on the Middle Atlantic Bight during 1979. Although the heating rate for the Middle Atlantic Bight cold eddy was a function of the distance the eddy travelled, Houghton *et al.* (1982) estimated that on average it was approximately between 0.5 °C and 2.0 °C per month. Based on a representative eddy temperature of about 4 °C a Newtonian heating timescale for the cold pool will be on the order of 10^7 s or about 3–4 months. It is possible to show (see §3.2) that this (eddy to slope water) mass conversion timescale is comparable with the timescale of the topographic Rossby waves induced by the vortex-tube compression in the slope water associated with the propagating eddy. We may expect, therefore, that the heating processes documented by Houghton *et al.* (1982) and Ou & Houghton (1982) will lead to a non-steady
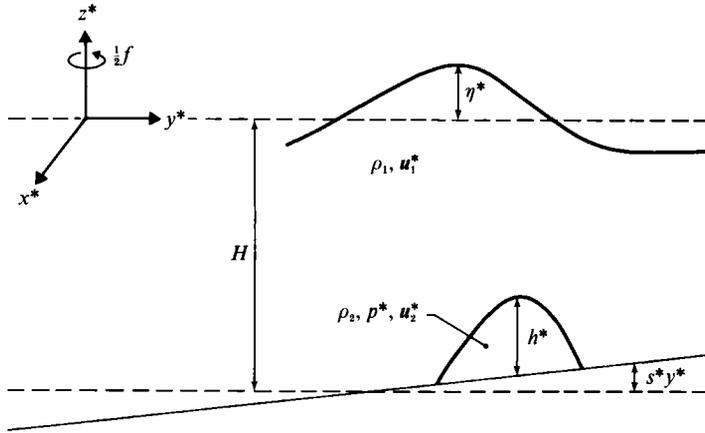
FIGURE 1. Geometry of the two-layer model used in this paper.

dynamical interaction between the cold eddy and the relatively warmer slope water involving diabatic heating, vortex-tube compression and the radiation of topographic Rossby waves.

In this paper a theory is developed to describe the propagation of a coherent cold-core eddy on a linearly sloping bottom. The theory will incorporate both dynamical interactions of the eddy with the surrounding fluid and ventilation processes. Based on 'synoptic' parameter values suggested by the oceanographic and experimental data, the new model equations that we derive to study the above processes correspond to strongly interacting 'hybrid' quasi-geostrophic, intermediate-lengthscale geostrophic dynamics (see Charney & Flierl 1981). Specifically, we argue that the dynamics of the surrounding slope water is essentially quasi-geostrophic but that the eddy dynamics while geostrophic is *not* quasi-geostrophic because eddy thickness changes are not small in comparison with the eddy-scale height itself. The above model is derived in a formal asymptotic expansion based on two-layer shallow-water theory assuming a small (appropriately scaled) shelf slope parameter.

The parameterization we adopt to describe the ventilation is the CI or cross-interfacial mass flux model of Dewar (1987, 1988a, b). Physically, this parameterization models the ventilation process as a continuous conversion of cold eddy water into relatively warmer slope water and is convenient for the two-layer model considered here. There have been other ventilation parameterizations suggested. For example, Chapman & Nof (1988) have proposed a parameterization for continuously stratified eddy models based on potential vorticity conservation principles.

The nonlinear model equations (see (3.14) and (3.15)) contain two non-dimensional parameters: an 'interaction' parameter (denoted μ) which physically measures the ratio of eddy-induced vortex-tube compression in the surrounding slope water to the background vorticity gradient associated with the shelf slope; and a diabatic heating parameter (denoted β) which measures the ratio of the timescale associated with the Nof translation speed to the ventilation timescale. In the absence of ventilation processes these equations admit an exact radially symmetric isolated-eddy slope-water solution which travels at the Nof speed and satisfies the Stern integral constraint (Mory 1985). However, the presence of the diabatic ventilation terms leads to temporal evolution in the eddy height which in turn, it is shown, leads to a weak topographic wave field in the slope water and a wave-drag-induced upslope drift in the propagating eddy.

The plan of the paper is as follows. In §2 the non-dimensional problem is formulated based on shallow-water theory and some preliminary remarks are made. In §3 the small-topographic-slope approximation is introduced and the 'quasi-geostrophic, intermediate lengthscale geostrophic' model is derived. In §4, the multiple-scale asymptotic theory is developed to describe the propagation and evolution of an initially isolated eddy due to the presence of ventilation processes and the subsequent emergence of the topographic wave field. In §5, the various salient features of our theory are illustrated with a simple example which assumes that the eddy has a parabolic configuration. The paper is summarized and some concluding remarks are made in §6.

2. Problem formulation

The basic model we assume is an f-plane two-layer system (both layers are assumed hydrostatic, homogeneous and incompressible) with a linearly varying bottom slope (see figure 1). The *dimensional* equations of motion for the upper layer or slope water (layer 1) can be written in the form

$$[\partial_{t^*} + \boldsymbol{u}_1^* \cdot \boldsymbol{\nabla}^*]\boldsymbol{u}_1^* + f\hat{\boldsymbol{e}}_3 \times \boldsymbol{u}_1^* + g\boldsymbol{\nabla}^*\eta^* = 0, \tag{2.1a}$$

$$(\eta^* - h^*)_{t^*} + \boldsymbol{\nabla}^* \cdot [\boldsymbol{u}_1^*(H + \eta^* - h^* - s^*y^*)] = -\mathscr{H}^*(x^*, y^*, t^*), \tag{2.1b}$$

where $\boldsymbol{u}_1^* = (u_1^*, v_1^*)$ is the horizontal velocity field, and f, g, η^*, h^*, H, and s^* are the constant Coriolis parameter, gravitational acceleration, reduced layer-1 pressure, cold dome thickness, 'mean' layer-1 thickness and bottom slope parameter, respectively. The dimensional coordinates are (x^*, y^*) and t^* is dimensional time. Subscripts x^*, y^* and t^* indicate partial differentiation, and $\boldsymbol{\nabla}^* = (\partial_{x^*}, \partial_{y^*})$. The term $-\mathscr{H}^*(x^*, y^*, t^*)$ in (2.1b) models the slope-water mass gain associated with the conversion of cold eddy water into relatively warmer slope water as a result of the diabatic processes. We will comment more completely on this term below.

The *dimensional* equations of motion describing the evolution of the cold-core eddy can be written in the form

$$[\partial_{t^*} + \boldsymbol{u}_2^* \cdot \boldsymbol{\nabla}^*]\boldsymbol{u}_2^* + f\hat{\boldsymbol{e}}_3 \times \boldsymbol{u}_2^* + \frac{1}{\rho_2}\boldsymbol{\nabla}^*p^* = 0, \tag{2.2a}$$

$$h_t^* + \boldsymbol{\nabla}^* \cdot [\boldsymbol{u}_2^* h^*] = \mathscr{H}^*(x^*, y^*, t^*), \tag{2.2b}$$

where the notation convention is similar to that used in (2.1), and where p^* is the dynamic pressure field in the eddy.

The diabatic heating of the cold pool is determined by the function $\mathscr{H}^*(x^*, y^*, t^*)$ in the eddy continuity equation (2.2b). Our parameterization for this term is based on the cross-interfacial (CI) model proposed by Dewar (1987, 1988a, b) for dynamically active warm rings given by

$$\mathscr{H}^*(x^*, y^*, t^*) = -\beta^*h^*. \tag{2.2c}$$

In this formulation (2.2c) is a simple Newtonian cooling/heating law which models the conversion of relatively colder eddy water to warmer slope water on a timescale determined by $1/\beta^*$. The reader is referred to Dewar (1987, 1988a, b) for a complete account of the physical principles for the model (2.2c). However, we point out here that this model implicitly assumes that the fluid must exist in either the cold-eddy density state or the relatively warmer slope-water density state. Accordingly, if the cold eddy is heated by the surrounding slope water an appropriate volume of eddy water is converted into slope water and, as a result, the effect of the warming will be to induce a mass loss in the cold eddy which is modelled by (2.2b, c). It is important

to add, however, that other eddy diabatic heating/cooling parameterizations have been suggested (e.g. Chapman & Nof 1988).

The system of equations (2.1) and (2.2) is closed with the requirement that the dynamic pressure be continuous across the eddy–slope-water interface, i.e.

$$p^* = \rho_1 g \eta^* + \rho_2 g'(h^* + s^* y^*), \qquad (2.3)$$

where ρ_1, ρ_2 and g' are the layer 1 and 2 densities, and the reduced gravity $g' = (\rho_2 - \rho_1)g/\rho_2 > 0$ (stable stratification), respectively.

Further analysis is facilitated by reformulating the governing equations into non-dimensional form. The non-dimensionalization scheme we adopt is motivated by (but is somewhat different from) the scalings used in Flierl (1984*b*). The non-dimensional (unasterisked) variables are given by

$$\begin{aligned}
(x^*, y^*) = L(x, y), \quad t^* = (fL/g's^*)\, t, \quad h^* = h_0 h, \\
u_1^* = \delta f L u_1, \quad \eta^* = \delta (fL)^2 g^{-1} \eta, \quad u_2^* = g's^* f^{-1} u_2, \\
p^* = \rho_2 L g's^* p,
\end{aligned} \qquad (2.4)$$

where $L = (g'H)^{\frac{1}{2}}/f$, $h_0 = h^*(x^* = y^* = t^* = 0)$ and $\delta = h_0/H$. The horizontal length-scale is the internal deformation radius and time has been scaled advectively based on the theoretical Nof translation speed. The scalings for u_1^* and η^* are based on the assumption that changes in upper-layer relative vorticity are due to vortex compression with u_1^* and η^* in geostrophic balance. As we will see, the above scalings will imply that the upper-layer dynamics will be quasi-geostrophic under a small-slope-parameter assumption. The lower-layer dynamics will be primarily geostrophic. The scaling for p^* is geostrophic and the scaling for u_2^* is the Nof translation speed. However, changes in the eddy thickness $h(x, y, t)$ will be as important as the horizontal divergence term $\nabla \cdot u_2$ in the continuity equation. Thus while momentum advection can be ignored for the eddy, the evolution of $h(x, y, t)$ is strongly coupled to u_2. These scalings are similar to those presented in Whitehead *et al.* (1990).

Substitution of (2.4) into (2.1), (2.2) and (2.3) gives the non-dimensional problem

$$su_{1_t} + \delta(u_1 \cdot \nabla)\, u_1 + \hat{e}_3 \times u_1 + \nabla \eta = 0, \qquad (2.5a)$$

$$s(h - g'\eta/g)_t + \nabla \cdot [u_1(\delta h + sy - 1 - g'\eta/g)] = -s\beta h, \qquad (2.5b)$$

$$su_{2_t} + s(u_2 \cdot \nabla)\, u_2 + \hat{e}_3 \times u_2 + \nabla p = 0, \qquad (2.5c)$$

$$h_t + \nabla \cdot (hu_2) = -\beta h, \qquad (2.5d)$$

$$(1 - g'/g)\, \delta\eta + \delta h + s(y - p) = 0, \qquad (2.5e)$$

where $\beta = \beta^*(fs)^{-1}$, and $s = s^*L/H$. We will estimate the magnitudes of δ, s and β in §3.2.

The following boundary conditions are imposed on the model. Suppose the projection of the intersection of the eddy with the sloping bottom on the plane $z = 0$ is given by $\phi(x, y, t) = 0$. The kinematic condition, which physically expresses the fact that a fluid parcel on the deforming eddy boundary remains on the boundary, is given by

$$\phi_t + u_2 \cdot \nabla \phi = 0 \quad \text{on} \quad \phi(x, y, t) = 0. \qquad (2.6)$$

The eddy thickness must satisfy

$$h(x, y, t) = 0 \quad \text{on} \quad \phi(x, y, t) = 0. \qquad (2.7)$$

For the upper layer we will impose the additional constraint that $r^{\frac{1}{2}}\eta \to 0$ as $r \to \infty$ 'ahead' of the propagating eddy. As pointed out by Miles (1968), this is the correct 'no upstream waves' condition (see also McKee 1971; McCartney 1975; Flierl 1984*a,b*).

3. Analysis for small topographic slope

3.1. *Modified Nof formulae*

It is possible to see how the theoretical expressions that Nof (1983) derived for the along-shelf and cross-shelf velocities are modified by the presence of a dynamically active upper layer as follows. Let us suppose that a steadily travelling ansatz can be made in the form $u_2 = u_2(\xi, \zeta)$, $h = h(\xi, \zeta)$, $\eta = \eta(\xi, \zeta)$ and $\phi = \phi(\xi, \zeta)$ with $\xi = x - c_x t$ and $\zeta = y - c_y t$ where $c = (c_x, c_y)$ is the translation velocity vector. In the absence of any diabatic processes, the eddy momentum and continuity equations can be written in the form

$$s^2[(u_2 - c) \cdot \nabla](u_2 - c) + s\hat{e}_3 \times u_2 + \nabla(\delta\eta + \delta h + s\zeta) = 0, \tag{3.1}$$

$$\nabla \cdot [h(u_2 - c)] = 0, \tag{3.2}$$

where $\nabla = (\partial_\xi, \partial_\zeta)$, respectively. The eddy boundary conditions (2.6) and (2.7) can be written in the respective forms,

$$\left. \begin{array}{r} (u_2 - c) \cdot \nabla\phi = 0, \\ h = 0, \end{array} \right\} \quad \text{on} \quad \phi(\xi, \zeta) = 0. \qquad \begin{array}{l} (3.3a) \\ (3.3b) \end{array}$$

If the product (3.1)·h is integrated over the eddy region $R = \{(\xi, \zeta) \,|\, \partial R = \phi\}$ it follows that

$$\iint_R \hat{e}_3 \times (hu_2) + \hat{e}_\zeta \iint_R h = -\frac{\delta}{s} \iint_R h\nabla\eta. \tag{3.4}$$

In deriving (3.4) we have already used the fact that the integral of $h(\xi, \zeta)$ times the nonlinear terms in (3.1) is identically zero since if we integrate by parts these terms it follows that

$$\iint_R h(u_2 - c) \cdot \nabla(u_2 - c) = \oint_{\phi=0} h(u_2 - c) \cdot n(u_2 - c) - \iint_R (u_2 - c) \nabla \cdot [h(u_2 - c)],$$

and the first term on the right-hand side is zero because of the boundary condition (3.3b) and the second term on the right-hand side is zero because of (3.2); see also Nof (1983).

From the continuity equation (3.2) we can infer the existence of a co-moving mass transport stream function $\psi = \psi(\xi, \zeta)$ satisfying

$$h(u_2 - c) = \hat{e}_3 \times \nabla\psi. \tag{3.5}$$

Note that it follows from (3.3a) that ψ is constant on $\phi = 0$, i.e. the eddy boundary forms a streamline in the co-moving frame of reference. Substituting (3.5) into (3.4) yields the relation

$$(\hat{e}_\zeta + \hat{e}_3 \times c) = -\frac{\delta}{s} \iint_R h\nabla\eta \,\Big/ \iint_R h. \tag{3.6}$$

It follows, immediately, that the components of the translation velocity vector will be given by

$$c_x = -1 - \frac{\delta}{s} \iint_R h\eta_\zeta \,\Big/ \iint_R h, \tag{3.7}$$

$$c_y = \frac{\delta}{s} \iint_R h\eta_\xi \,\Big/ \iint_R h. \tag{3.8}$$

In the no interaction limit $(\delta \to 0)$, these expressions reduce exactly to the Nof formulae.

3.2. *Approximation of small topographic slope*

The modified Nof formulae (3.7) and (3.8) state that the interaction between the eddy and the surrounding fluid is $O(\delta/s)$ in comparison with the leading-order (non-interaction) terms. In this section we shall examine the small-slope asymptotic limit defined by

$$\delta = \mu s, \tag{3.9}$$

where $0 < s \ll 1$ and $\mu = O(1)$. This limit will correspond to a strongly interacting eddy–slope water configuration in the sense that although $0 < s \approx \delta \ll 1$ the fact that $\mu = O(1)$ in $(2.5e)$ will mean that the leading-order dynamics for the eddy height cannot be decoupled from the dynamics for the geostrophic pressure in the slope water (see (3.14)). Physically, this limit has a simple interpretation. The scaled topographic slope parameter $s = s^*L/H$ can be rearranged into the form $s = (s^*g'/f)/(g'H)^{\frac{1}{2}}$. Thus the parameter s can be interpreted as the ratio of the Nof speed to the phase or group speed of the long baroclinic gravity wave solutions in the model. The limit $s \to 0^+$ can be viewed as a low-bandpass filter which will effectively remove the long baroclinic gravity waves in the slope water and focus attention on the vorticity wave processes.

The observations reported in Armi & D'Asaro (1980) and Houghton *et al.* (1982) suggest that the small (non-dimensional)-slope approximation and the scaling (3.9) are physically relevant. For example, the observations of the cold pool reported by Houghton *et al.* (1982) correspond to approximate parameter values of $s^* \approx 1.2$ m/km, $L \approx 15$ km, $h_0 \approx 30$–40 m and $H \approx 200$–300 m suggesting $s \approx 4 \times 10^{-2}$, $\delta \approx 2 \times 10^{-2}$ and consequently that $\mu = O(1)$. The oceanographic observations of Armi & D'Asaro and the rotating-tank data of Mory *et al.* scale similarly. The magnitude of the non-dimensional heating parameter β can be estimated as follows. Based on a heating rate of about 2 °C/month and a scale eddy temperature of 4 °C, it follows that $\beta^* \approx 2 \times 10^{-7}$ s^{-1}. Based on $f \approx 10^{-4}$ s^{-1} and $s \approx 4 \times 10^{-2}$ it therefore follows that $\beta = \beta^*(fs)^{-1} \approx 10^{-1}$. Consequently, as a rough first approximation, we see that $s \approx \delta$ and that heating processes, while relatively weak, are an order of magnitude larger than the ageostrophic terms in the eddy momentum balance.

Substitution of (3.9) into (2.5) yields the following set of equations for the eddy and surrounding slope-water problem:

$$\hat{\boldsymbol{e}}_3 \times \boldsymbol{u}_1 + \boldsymbol{\nabla}\eta = -s\boldsymbol{u}_{1_t} - s\mu(\boldsymbol{u}_1 \cdot \boldsymbol{\nabla})\boldsymbol{u}_1, \tag{3.10a}$$

$$\boldsymbol{\nabla} \cdot \boldsymbol{u}_1 = sh_t + s\boldsymbol{\nabla} \cdot (y\boldsymbol{u}_1) + \mu s\boldsymbol{\nabla} \cdot (h\boldsymbol{u}_1) + s\beta h, \tag{3.10b}$$

$$\hat{\boldsymbol{e}}_3 \times \boldsymbol{u}_2 + \hat{\boldsymbol{e}}_2 + \mu\boldsymbol{\nabla}(h + \eta) = -s\boldsymbol{u}_{2_t} - s(\boldsymbol{u}_2 \cdot \boldsymbol{\nabla})\boldsymbol{u}_2, \tag{3.11a}$$

$$h_t + \boldsymbol{\nabla} \cdot (h\boldsymbol{u}_2) = -\beta h, \tag{3.11b}$$

subject to the eddy boundary conditions

$$\left.\begin{aligned}\phi_t + (\boldsymbol{u}_2 \cdot \boldsymbol{\nabla})\phi &= 0, \\ h(x, y, t) &= 0,\end{aligned}\right\} \quad \text{on} \quad \phi(x, y, t) = 0, \tag{3.12a}$$
$$\tag{3.12b}$$

and the appropriate radiation condition. In (3.10b) we have neglected those terms in (2.5b) which are $O(\eta g'/g)$. The elimination of these terms will filter the long surface gravity waves out of the model.

The location of the slope parameter s in (3.10) occurs in such a way that to $O(s)$ the dynamics of the shelf water will be quasi-geostrophic. The location of the slope

parameter s in (3.11 a, b) implies that the interior eddy dynamics is essentially geostrophic but not quasi-geostrophic since changes in h are comparable with h itself. This is analogous to the 'intermediate lengthscale dynamics' identified in Charney & Flierl (1981).

We can exploit the fact that $0 < s \ll 1$ by constructing a straightforward asymptotic expansion of the form

$$(\eta, p, \boldsymbol{u}_1, \boldsymbol{u}_2, h, \phi) \sim (\eta_0, p_0, \boldsymbol{u}_{10}, \boldsymbol{u}_{20}, h_0, \phi_0) + s(\eta_1, p_1, \boldsymbol{u}_{11}, \boldsymbol{u}_{21}, h_1, \phi_1) + \dots. \quad (3.13)$$

Substitution of this expansion into (3.10), (3.11) and (3.12) yields the $O(1)$ problem in the form

$$(\nabla^2 \partial_t + \partial_x)\eta_0 + h_{0_x} + \mu J(\eta_0, \nabla^2 \eta_0) = 0, \quad (3.14a)$$

$$h_{0_t} - h_{0_x} + \mu J(\eta_0, h_0) = -\beta h_0. \quad (3.14b)$$

The quasi-geostrophic potential vorticity equation (3.14a) is obtained in the usual way (see e.g. Pedlosky 1987, §3.12), by forming the vorticity equation for the $O(s)$ equations associated with (3.10a), eliminating the $O(s)$ divergence term using (3.10b), and then finally simplifying the resulting expression using the $O(1)$ equations obtained from (3.11).

The leading-order velocities and dynamic pressure in the eddy will be obtained from the auxiliary relations

$$\boldsymbol{u}_{10} = \hat{\boldsymbol{e}}_3 \times \boldsymbol{\nabla}\eta_0, \quad (3.15a)$$

$$\boldsymbol{u}_{20} = -\hat{\boldsymbol{e}}_1 + \mu\hat{\boldsymbol{e}}_3 \times \boldsymbol{\nabla}(\eta_0 + h_0), \quad (3.15b)$$

$$p_0 = y + \mu(\eta_0 + h_0), \quad (3.15c)$$

and the eddy boundary conditions can be written in the form

$$\left.\begin{aligned}\phi_{0_t} - \phi_{0_x} + \mu J(\eta_0 + h_0, \phi_0) = 0, \\ h_0 = 0,\end{aligned}\right\} \quad \text{on} \quad \phi_0 = 0, \quad \begin{aligned}(3.16a) \\ (3.16b)\end{aligned}$$

where the Jacobian is given by $J(A, B) = A_x B_y - A_y B_x$.

The problem posed by the set of equations (3.14) retains all of the physics associated with the Nof and Mory *et al.* theories. If we were to introduce (as we eventually will in a suitable form) co-moving coordinates $\xi = x - c_x t$ and $\zeta = y - c_y t$ into (3.14) (with $\beta = 0$) and multiply (3.14b) by ξ and integrate over the eddy region R, the result would be the generalized Nof formula (3.7). Similarly, multiplying (3.14b) by ζ and integrating over R would yield (3.8).

The model of Ou & Houghton (1982) for the along-shelf heating of the Middle Atlantic Cold Pool can be viewed as corresponding to (3.14b) with η_0 as a prescribed geostrophic pressure associated with a steady along-shelf current and the additional approximation $h_{0_y} \ll h_{0_x}$. In Ou & Houghton's theory the slope water does not dynamically evolve and thus there is no analogue of (3.14a) in their model. The equations (3.14a, b) without the heating terms have also been derived in Whitehead *et al.* (1989). Their analysis develops an integral constraint for isolated cold eddies and a lower bound for the eddy radius. Although no explicit analytical solutions are presented, a series of numerical experiments is described.

Earlier in this section we argued that, based on observed order of magnitude estimates for our scalings, the interaction parameter $\mu = O(1)$. Consequently, (3.14)–(3.16) constitute a fully interacting coupled eddy–slope water model. We have not been able to find a *general* solution for these equations for arbitrary initial conditions. However, exact nonlinear solutions can be obtained for some special cases. For example, in the absence of any diabatic processes (i.e. $\beta = 0$) we can find exact radially symmetric non-radiating steadily travelling solutions (described in the next section).

4. Weak diabatic heating theory

4.1. *Problem formulation*

Although we have not been able to find a *general* solution to (3.14) and (3.16), it is possible to make further progress under a weak diabatic heating limit. In our discussion in §3.2 it was argued that the interaction parameter $\mu = O(1)$ but that $\beta = O(10^{-1})$. In this Section we shall develop a theory describing the dynamical evolution of an isolated eddy and slope-water configuration, which is initially balanced so that there is no fully developed $O(1)$ wave field in the slope water for $t \approx 0^+$, under the asymptotic limit $0 \ll s \ll \beta \ll 1$. We shall show that the vortex-tube dynamics associated with the diabatic mass conversion will result in the generation of topographic Rossby waves in the slope water and an induced upslope motion in the propagating eddy.

Assuming the cold-core eddy is to leading order radially symmetric, it is natural to reformulate the governing equations in the co-moving polar coordinates $r = (\xi^2 + \zeta^2)^{\frac{1}{2}}$ and $\theta = \tan^{-1}(\zeta/\xi)$, and the slow time $T = \beta t$, where ξ and ζ are the co-moving phase variables

$$\xi = x - \beta^{-1} \int_0^{\beta t} c_x(t') \, \mathrm{d}t', \tag{4.1a}$$

$$\zeta = y - \beta^{-1} \int_0^{\beta t} c_y(t') \, \mathrm{d}t'. \tag{4.1b}$$

Note that the along-shelf and cross-shelf velocities given by $-\xi_t = c_x(T)$ and $-\zeta_t = c_y(T)$ respectively have both been formally scaled $O(1)$ on account of the assumption that $\mu = O(1)$ in (3.7) and (3.8). As it turns out, however, the assumption that the leading-order eddy and slope-water configuration contains no wave field will imply that $c_y = O(\beta)$. We have also allowed the translation speeds to be time dependent on the slow timescale $O(\beta^{-1})$ because of the presence of the diabatic heating terms.

It follows from (4.1) that derivatives in the governing equations will map according to

$$\partial_x \rightarrow \cos(\theta) \, \partial_r - r^{-1} \sin(\theta) \, \partial_\theta, \tag{4.2a}$$

$$\partial_y \rightarrow \sin(\theta) \, \partial_r + r^{-1} \cos(\theta) \, \partial_\theta, \tag{4.2b}$$

$$\partial_t \rightarrow -c_x(T)[\cos(\theta) \, \partial_r - r^{-1} \sin(\theta) \, \partial_\theta] - c_y(T)[\sin(\theta) \, \partial_r + r^{-1} \cos(\theta) \, \partial_\theta] + \beta \, \partial_T. \tag{4.2c}$$

As well, the boundary of the eddy will be written in the form

$$\phi(x, y, t) = r - a(\theta, T) = 0.$$

Substitution of (4.2) and the assumed form for the eddy boundary into (3.14), (3.15) and (3.16) yields

$$[\cos(\theta) \, \partial_r - r^{-1} \sin(\theta) \, \partial_\theta][-c_x \nabla^2 \eta + \eta + h] + \mu J(\eta, \nabla^2 \eta)$$
$$- c_y[\sin(\theta) \, \partial_r + r^{-1} \cos(\theta) \, \partial_\theta] \nabla^2 \eta = -\beta \nabla^2 \eta_T, \tag{4.3}$$

$$(c_x + 1)[\cos(\theta) \, \partial_r - r^{-1} \sin(\theta) \, \partial_\theta] h - \mu J(\eta, h)$$
$$+ c_y[\sin(\theta) \, \partial_r + r^{-1} \cos(\theta) \, \partial_\theta] h = \beta h_T + \beta h, \tag{4.4}$$

subject to the eddy boundary conditions

$$h = 0, \tag{4.5a}$$

$$(c_x + 1)[a \sin(\theta)]_\theta - c_y[a \cos(\theta)]_\theta = -\mu a_\theta(\eta + h)_r - \mu(\eta + h)_\theta - \beta a a_T, \tag{4.5b}$$

evaluated on $r = a(\theta, T)$. In polar coordinates, the Jacobian takes the form

$J(A, B) = r^{-1}(A_r B_\theta - A_\theta B_r)$ and $\nabla^2 = \partial_{rr} + r^{-1}\partial_r + r^{-2}\partial_{\theta\theta}$. Note that we have deleted the zero subscript from the dependent variables for subsequent notational convenience.

The radiation condition on the slope-water geostrophic pressure can be written in the form

$$\lim_{r \to \infty} r^{\frac{1}{2}} \eta(r, \theta; T) = 0, \tag{4.6}$$

in the sector $|\theta - \theta_*| < \frac{1}{2}\pi$ where $\theta_* = \tan^{-1}(c_y/c_x)$. This condition is obtained as follows. The slowly modulated eddy will propagate along a path whose tangent vector is given by $(c_x(T), c_y(T))$ on the (x, y)-coordinate plane at each instant of time. The velocity vector will form an angle $\theta_* = \tan^{-1}(c_y/c_x)$ with the positive x-axis. Defining 'ahead' of the propagating eddy to be those coordinates with angle θ satisfying $-\frac{1}{2}\pi < \theta - \theta_* < \frac{1}{2}\pi$, then the 'no waves' constraint that $r^{\frac{1}{2}}\eta \to 0$ as $r \to \infty$ ahead of the propagating eddy (see Miles 1968 or Flierl 1984b) can be written as above.

4.2. *The leading-order solution*

We shall develop a weakly ventilated theory for an initially radially symmetric isolated baroclinic eddy. The (formal) asymptotic expansion is given by

$$h(r, \theta; T) = h^{(0)}(r; T) + \beta h^{(1)}(r, \theta; T) + \dots, \tag{4.7a}$$

$$\eta(r, \theta; T) = \eta^{(0)}(r; T) + \beta \eta^{(1)}(r, \theta; T) + \dots, \tag{4.7b}$$

$$a(\theta; T) = a^{(0)}(T) + \beta a^{(1)}(\theta; T) + \dots, \tag{4.7c}$$

$$c_x(T) = c_x^{(0)}(T) + O(\beta^2), \tag{4.7d}$$

$$c_y(T) = c_y^{(0)}(T) + \beta c_y^{(1)}(T) + O(\beta^2). \tag{4.7e}$$

As well, the eddy boundary conditions (4.5a, b) will have to be Taylor expanded about $r = a^{(0)}(T)$. Neglecting terms of $O(\beta^3)$ and higher, the approximate boundary conditions associated with (4.5a, b) can be written in the respective forms

$$h + (a - a^{(0)}) h_r + \tfrac{1}{2}(a - a^{(0)})^2 h_{rr} + O(\beta^3) = 0, \tag{4.8a}$$

$$(c_x + 1)[a \sin(\theta)]_\theta - c_y[a \cos(\theta)]_\theta = -\mu a_\theta(\eta + h)_r - \mu(\eta + h)_\theta - \beta a a_T$$
$$- \mu a_\theta(a - a^{(0)})(\eta + h)_{rr} - \mu(a - a^{(0)})(\eta + h)_{\theta r} + O(\beta^3), \tag{4.8b}$$

evaluated on $r = a^{(0)}(T)$.

In the expansion for the along-shelf translation speed $c_x(T)$ given in (4.7d) we have implicitly assumed $c_x^{(1)}(T) = 0$. It turns out that if this term is retained in the asymptotic expansion it is possible to formally determine completely the $O(\beta)$ solutions (in particular the exterior wave field) *and* satisfy all known solvability conditions associated with the $O(\beta)$ equations with this parameter left unspecified. We have therefore chosen to set $c_x^{(1)}(T) = 0$. We hasten to add that it may be that $c_x^{(1)}(T)$ is determined from solvability conditions associated with the $O(\beta^2)$ or higher-order problems. However, our inability to solve the $O(\beta)$ equations for the eddy in closed form for even the simplest $h^{(0)}$ and $\eta^{(0)}$ has not made this determination tractable. This is unfortunate because the experiments carried out by Mory *et al.* (1987) showed that the observed along-shelf translation speed of the eddy was much smaller than the Nof speed and we have not been able to reproduce this result for an eddy subjected to diabatic heating. (Recent informal discussions with D. Nof and M. Stern suggest that errors in the measuring of the eddy density may have led to overestimating the appropriate Nof speed for the Mory *et al.* experiment and as a result the discrepancy may not be nearly as large as originally thought.)

Substitution of the expansion (4.7) into (4.3), (4.4) and (4.8) yields the $O(1)$ set of equations

$$\cos(\theta)[-c_x^{(0)} \nabla^2 \eta^{(0)} + \eta^{(0)} + h^{(0)}]_r - c_y^{(0)} \sin(\theta) \nabla^2 \eta_r^{(0)} = 0, \qquad (4.9a)$$

$$[(c_x^{(0)} + 1)\cos(\theta) + c_y^{(0)} \sin(\theta)] h_r^{(0)} = 0, \qquad (4.9b)$$

subject to the $O(1)$ boundary conditions

$$h^{(0)}[a^{(0)}(T); T] = 0, \qquad (4.10a)$$

$$[\cos(\theta)(c_x^{(0)} + 1) + c_y^{(0)} \sin(\theta)] a^{(0)} = 0. \qquad (4.10b)$$

Assuming a non-trivial solution for $h^{(0)}$ and $a^{(0)}$, it follows directly from (4.9b) or (4.10b) and the orthogonality of the trigonometric functions over $0 < \theta < 2\pi$ that

$$c_x^{(0)} = -1, \quad c_y^{(0)} = 0, \qquad (4.11a, b)$$

and consequently from (4.9a) that

$$\nabla^2 \eta^{(0)} + \eta^{(0)} = -h^{(0)}, \qquad (4.12)$$

where the constant of integration is zero because the eddy is isolated.

Note that $h^{(0)}(r; T)$ is undetermined to this order except for the boundary condition (4.10a). The fact that $h^{(0)}(r, T)$ is undetermined at this order is a difficulty which occurs in many models of isolated eddies (e.g. Killworth 1983; Nof 1983; Flierl 1984b, among others). Flierl (1984b) chose to close the problem by specifying the potential vorticity distribution in the eddy interior which in turn would uniquely determine $h^{(0)}(r; T)$. Nof (1983) preferred to specify the interior eddy *swirl* velocity (i.e. the eddy azimuthal velocity in a frame of reference moving with the along-shelf Nof speed) and thereby determine the appropriate corresponding eddy height. Here, it will be more convenient to specify $h^{(0)}(r; 0)$ and simply compute the other corresponding fields. However, because of our scaling, we can interpret the specification of $h^{(0)}(r; 0)$ as equivalent to a potential vorticity specification in the following sense. The potential vorticity associated with (2.5c) and (2.5d) may be written in the form $P = [s\hat{e}_3 \cdot (\nabla \times u_2) + 1]/h$. Thus in the limit as $s \to 0$ we have $P \approx 1/h_0 + O(s)$. Consequently in the small-slope limit adopted here, the specification of h_0 is equivalent to a specification of the leading-order potential vorticity.

Given the leading-order eddy height $h^{(0)}(r; T)$, the *isolated* solution for the geostrophic pressure in the surrounding slope water can be written in the form (see Flierl 1984b)

$$\eta^{(0)}(r; T) = -\tfrac{1}{2}\pi Y_0(r) \int_0^r r' J_0(r') h^{(0)}(r'; T)\, dr' - \tfrac{1}{2}\pi J_0(r) \int_r^{a^{(0)}} r' Y_0(r') h^{(0)}(r'; T)\, dr',$$
$$(4.13a)$$

in $r \leqslant a^{(0)}$, and
$$\eta^{(0)}(r; T) = 0, \qquad (4.13b)$$

in $r > a^{(0)}$, with the 'isolation' constraint

$$\int_0^{a^{(0)}} r J_0(r) h^{(0)}(r; T)\, dr = 0. \qquad (4.13c)$$

The constraint (4.13c) is the necessary and sufficient condition for the annihilation of the external topographic wave field (Flierl 1984a) and can be physically interpreted as a zero-wave drag condition. It also follows from (4.13c) that the relative circulation in the upper layer is zero and that $\eta_r^{(0)}(a^{(0)}; T) = 0$.

The condition (4.13c) will imply that the allowed leading-order eddy radius can only take on a discrete set of values determined by the particular form for $h^{(0)}(r; T)$.

The no radiation condition (4.13c) raises an interesting issue concerning the characterization or determination of the class of functions $h^{(0)}(r;T)$ that will allow (4.13c) to have non-trivial solutions ($a^{(0)} = 0$ is always a solution). For example, if we take $h^{(0)}(r;0) = J_0(r)$ it immediately follows that *only* $a^{(0)} = 0$ is allowed. We have been unable to determine general necessary and sufficient conditions on $h^{(0)}(r;T)$ which will guarantee that non-trivial solutions for $a^{(0)}$ exist and this aspect of our theory remains problematic. The constraint (4.13c) may be viewed as resulting from the fact that the leading-order time evolution is modelled solely as the result of quasi-steady advection (see (4.2c)). This assumption will remove the possibility of generating an $O(1)$ wave field during the early adjustment period that would occur in a true initial-value problem. Accordingly, it is important to emphasize again that the theory developed here is only valid for an appropriately adjusted or dynamically balanced initial eddy–slope water configuration which can satisfy the $O(1)$ zero-wave-drag condition. We would also like to comment here that the eddy–slope-water solution configuration just obtained can be interpreted as corresponding to a steadily travelling baroclinic monopole on a continental shelf.

The leading-order isolated eddy solution just constructed will satisfy the *Stern integral constraint* for isolated eddies (Mory 1983, 1985), which for our theory can be expressed in the form

$$\int_0^{a^{(0)}} r[\eta^{(0)}(r;T) + h^{(0)}(r;T)]\,\mathrm{d}r = 0. \qquad (4.14)$$

This result follows immediately from (4.12) and the fact that $\eta_r^{(0)}(a^{(0)};T) = 0$ as a consequence of (4.13).

Stern's integral constraint has an interesting consequence for the eddy swirl velocity (i.e. the eddy azimuthal velocity relative to the steady along-shelf Nof translation speed) distribution. It follows from (3.15c) that the leading-order eddy swirl velocity, denoted by $v_s(r;T)$, is given by

$$v_s(r;T) = \mu(\eta^{(0)} + h^{(0)})_r. \qquad (4.15)$$

However, from (4.14) and (4.15) it is easy to show that

$$\int_0^{a^{(0)}} r^2 v_s(r;T)\,\mathrm{d}r = 0. \qquad (4.16)$$

Clearly the constraint (4.16) will imply that within the eddy there must be regions of cyclonic *and* anticyclonic circulation if there is to be any swirl velocity at all. At first this result may seem counter-intuitive because it is natural to think that the swirl velocity in a cold-core eddy would be strictly anticyclonic. But this conclusion rests on the assumption that the dynamic pressure in the eddy is relatively unaffected by the dynamical response of the surrounding slope water. However, the theory presented here suggests (see (3.15c)) that the contribution to the eddy dynamic pressure from the slope-water geostrophic pressure and the eddy thickness are comparable. Since $\eta_r^{(0)} < 0$ where $h_r^{(0)} > 0$ (i.e. flow above the eddy is cyclonic), it can easily follow from (3.15c) that the eddy swirl velocity can take on positive as well as negative values. We shall illustrate these points with an example calculation in §5.

4.3. *The first-order perturbation equations*

There are several dynamical characteristics of the leading order solution that have yet to be determined and for which we will have to examine the $O(\beta)$ equations of motion. We shall be able to determine, based on relatively direct solvability

conditions on the $O(\beta)$ equations, the slow-time ventilation of the cold eddy as well as the leading-order cross-shelf translation velocity. Also, the $O(\beta)$ exterior topographic wave field in the slope water can be determined.

The $O(\beta)$ problem in the eddy region $r < a^{(0)}$ can be written in the form

$$[\cos(\theta)\,\partial_r - r^{-1}\sin(\theta)\,\partial_\theta][\nabla^2\eta^{(1)} + \eta^{(1)} + h^{(1)}] - \mu\eta_\theta^{(1)}\nabla^2\eta_r^{(0)}/r + \mu\eta_r^{(0)}\nabla^2\eta_\theta^{(1)}/r$$
$$= c_y^{(1)}\sin(\theta)\nabla^2\eta_r^{(0)} - \nabla^2\eta_T^{(0)}, \qquad (4.17a)$$

$$c_y^{(1)}\sin(\theta)\,h_r^{(0)} - \mu r^{-1}[\eta_r^{(0)}h_\theta^{(1)} - \eta_\theta^{(1)}h_r^{(0)}] = h_T^{(0)} + h^{(0)}, \qquad (4.17b)$$

subject to the $O(\beta)$ eddy boundary conditions

$$h^{(1)}(a^{(0)}, \theta; T) + h_r^{(0)}(a^{(0)}; T)\,a^{(1)}(\theta; T) = 0, \qquad (4.18a)$$

$$\mu\eta_\theta^{(1)} = -c_y^{(1)}a^{(0)}\sin(\theta) - a^{(0)}a_T^{(0)}, \qquad (4.18b)$$

evaluated on $r = a^{(0)}$, where $(4.18a)$ and $\eta_r^{(0)}(a^{(0)}, T) = 0$ has been used to obtain $(4.18b)$.

In the region *exterior* to the eddy (i.e. $r > a^{(0)}$) the upper-layer geostrophic pressure satisfies

$$\nabla^2\eta^{(1)} + \eta^{(1)} = 0, \qquad (4.19)$$

where, again, the constant of integration has been set to zero because it is assumed that $\eta^{(1)} \to 0$ as $r \to \infty$.

The leading-order response of the eddy to the diabatic heating is determined by $(4.17b)$. Because of the orthogonality of the trigonometric functions and the periodicity that $\eta^{(1)}$ and $h^{(1)}$ must have over the interval $0 < \theta < 2\pi$, it follows from $(4.17b)$ that

$$h_T^{(0)} + h^{(0)} = 0. \qquad (4.20)$$

Similarly it follows from $(4.18b)$ that $a_T^{(0)} = 0$. The solution to (4.20) is given by simply

$$h^{(0)}(r; T) = \tilde{h}(r)\exp(-T), \qquad (4.21)$$

where $\tilde{h}(r)$ corresponds to the initial radially symmetric eddy height profile.

4.3.1. *Determination of the cross-shelf translation speed*

Even for a very simple $O(1)$ eddy height configuration (e.g. $h^{(0)}(r; 0)$ given as a parabola; see §5), the $O(\beta)$ eddy problem cannot be solved exactly and a numerical solution will be required. However, as it turns out, detailed knowledge of the structure of $h^{(1)}(r, \theta; T)$ and $\eta^{(1)}(r, \theta; T)$ is *not* required in order to determine either the leading-order cross-shelf translation speed or the complete structure of the exterior (i.e. $r > a^{(0)}$) topographic wave field.

The simplest and most direct way to obtain $c_y^{(1)}(T)$ is to work directly with (4.17) rewritten in the co-moving Cartesian variables (ξ, ζ) given by (4.1). In these coordinates (4.17) can be written in the form

$$[\nabla^2\eta^{(1)} + \eta^{(1)} + h^{(1)}]_\xi + \mu J(\eta^{(0)}, \nabla^2\eta^{(1)}) + \mu J(\eta^{(1)}, \nabla^2\eta^{(0)}) = c_y^{(1)}\nabla^2\eta_\zeta^{(0)} - \nabla^2\eta_T^{(0)}, \quad (4.22)$$

$$\mu J(\eta^{(0)}, h^{(1)}) + \mu J(\eta^{(1)}, h^{(0)}) = c_y^{(1)}h_\zeta^{(0)} - h^{(0)} - h_T^{(0)}. \qquad (4.23)$$

In order to obtain solvability conditions on (4.22) and (4.23) we shall have to examine homogeneous solutions of the adjoint problem associated with (4.22) and (4.23). The procedure we describe here is similar to that developed by Flierl $(1984b)$.

The governing equations for the adjoint problem can be obtained by multiplying (4.22) by a function $\phi_1(\xi, \zeta; T)$ and multiplying (4.23) by a function $\phi_2(\xi, \zeta; T)$, adding

the two expressions together and then integrating over the eddy region. The result can be put into the form

$$\iint_R [\mu J(h^{(0)}, \phi_2) - \mu \nabla^2 J(\eta^{(0)}, \phi_1) - \mu J(\eta^{(0)} + h^{(0)}, \phi_1) - \partial_\xi (\nabla + 1) \phi_1)] \eta^{(1)} \, d\xi \, d\zeta$$

$$- \iint_R [\mu J(\eta^{(0)}, \phi_2) + \partial_\xi \phi_1] h^{(1)} \, d\xi \, d\zeta$$

$$= \iint_R [c_y^{(1)} \nabla^2 \eta_\xi^{(0)} - \nabla^2 \eta_T^{(0)}] \phi_1 \, d\xi \, d\zeta + \iint_R [c_y^{(1)} h_\xi^{(0)} - h^{(0)} - h_T^{(0)}] \phi_2 \, d\xi \, d\zeta, \qquad (4.24)$$

assuming where necessary that the boundary integrals are zero.

The homogeneous adjoint problem will therefore be given by

$$\mu J(h^{(0)}, \phi_2) - \mu \nabla^2 J(\eta^{(0)}, \phi_1) - \mu J(\eta^{(0)} + h^{(0)}, \phi_1) - \partial_\xi (\nabla^2 + 1) \phi_1 = 0, \qquad (4.25)$$

$$\mu J(\eta^{(0)}, \phi_2) + \partial_\xi \phi_1 = 0. \qquad (4.26)$$

We can find three immediate homogeneous solutions: $(\phi_1 = 0, \phi_2 = 1)$, $(\phi_1 = 1, \phi_2 = 0)$ and $(\phi_1 = -\eta^{(0)}, \phi_2 = \zeta/\mu)$. There may be other solutions but we have not been able to find them. When these homogeneous solutions are substituted into (4.24) the left-hand side is identically zero and the right-hand side gives us the required solvability conditions. From the pair $(\phi_1 = 0, \phi_2 = 1)$ we find

$$\iint_R [h_T^{(0)} + h^{(0)}] \, d\xi \, d\zeta = 0, \qquad (4.27)$$

which is satisfied on account of (4.20). From the pair $(\phi_1 = 1, \phi_2 = 0)$ we find

$$\iint_R \nabla^2 \eta_T^{(0)} \, d\xi \, d\zeta = 0, \qquad (4.28)$$

which is satisfied because $\eta_r^{(0)}(a^{(0)}; T) = 0$. From the pair $(\phi_1 = -\eta^{(0)}, \phi_2 = \zeta/\mu)$ we find

$$c_y^{(1)} \iint_R h^{(0)} \, d\xi \, d\zeta = \mu \iint_R \eta^{(0)} \nabla^2 \eta_T^{(0)} \, d\xi \, d\zeta,$$

which can be rearranged using (4.14) into the form

$$c_y^{(1)}(T) = \tfrac{1}{2}\mu \, \partial_T \int_0^{a^{(0)}} r[\nabla \eta^{(0)} \cdot \nabla \eta^{(0)}](r; T) \, dr \Big/ \int_0^{a^{(0)}} r \eta^{(0)}(r; T) \, dr. \qquad (4.29)$$

It follows from (4.29) that $c_y^{(1)}(T) > 0$ since the numerator and denominator are both negative definite. This can be shown as follows. From (4.14) and the fact that $h^{(0)}(r; T) \geqslant 0$ for $0 \leqslant r \leqslant a^{(0)}$ it will follow that the denominator in (4.29) is negative. If (4.21) is substituted into (4.13a) then it follows that $\eta^{(0)}(r; T)$ will have the general form $\eta^{(0)}(r; T) = \tilde{\eta}(r) \exp(-T)$, where $\tilde{\eta}(r)$ is a radially symmetric function that is determined in the calculation of (4.13a). Substituting this form for $\eta^{(0)}(r; T)$ into the numerator of (4.29) yields a term of the form $\partial_T[\eta_* \exp(-2T)]$ where the constant $\eta_* > 0$ and hence the numerator will also be negative. Thus the effect of ventilation is to induce *upslope* motion in the propagating eddy. As the process of ventilation continues (4.29) implies that the magnitude of cross-shelf drift speed will decrease since the magnitude of $\eta^{(0)}$ decreases as T increases.

This qualitative result can be interpreted as a consequence of the conservation of potential vorticity in the upper layer. Equations (3.14a) and (3.14b) can be combined

to state that to leading order in β the potential vorticity $\nabla^2 \eta + h + y$ is conserved following the geostrophic motion. Since the leading-order 'averaged' geostrophic vorticity or circulation in the slope water above the eddy is identically zero, the effect of the diabatic heating (which implies $h_t < 0$) can only be offset by a corresponding increase in the mean cross-shelf position of the cold-core eddy.

4.3.2. *Determination of the exterior topographic wave field*

The $O(\beta)$ geostrophic pressure in the exterior region for the upper layer must satisfy

$$\nabla^2 \eta^{(1)} + \eta^{(1)} = 0, \tag{4.30}$$

subject to the boundary condition

$$\eta^{(1)} = \mu^{-1} c_y^{(1)} \cos(\theta), \tag{4.31a}$$

evaluated on $r = a^{(0)}$, and the no-upstream-waves condition

$$r^{\frac{1}{2}} \eta^{(1)}(r, \theta; T) \to 0 \quad \text{as} \quad r \to \infty \quad \text{in} \quad \tfrac{1}{2}\pi < \theta < \tfrac{3}{2}\pi. \tag{4.31b}$$

The boundary condition (4.31a), which follows directly from (4.18b), will ensure that the geostrophic pressure and normal mass flux in the slope water is continuous across the eddy boundary $r = a^{(0)}$.

The method of solution we use is a modification of the procedures developed by Miles (1968) for a similar boundary-value problem (see also McKee 1971; McCartney 1975; Flierl 1984a). Following the arguments presented in Miles we construct the exterior geostrophic pressure field in the form

$$\eta^{(1)} = \sum_{n=0}^{\infty} a_n(T) [Y_n(r) \cos(n\theta) + \psi_n(r, \theta; T)] / Y_n(a^{(0)}), \tag{4.32a}$$

where

$$\psi_n(r, \theta; T) = \sum_{m=0}^{\infty} b_{n,m} J_m(r) \cos(m\theta). \tag{4.32b}$$

(The reason for our particular choice of normalization in (4.32a) will be given below.)

Recalling that the even (odd) $J_n(r)$ functions have the same asymptotic form as the odd (even) $Y_n(r)$ functions as $r \to \infty$ (see Abramowitz & Stegun 1965), the no-waves condition (4.31b) will imply that the coefficients $b_{n,m}$ must satisfy the constraints

$$\cos(2n\theta) = \sum_{m=0}^{\infty} (-1)^{m+n+1} b_{2n, 2m+1} \cos[(2m+1)\theta], \tag{4.33a}$$

$$\cos[(2n+1)\theta] = \sum_{m=0}^{\infty} (-1)^{m+n} b_{2n+1, 2m} \cos[2m\theta], \tag{4.33b}$$

for $n = 0, 1, 2, \ldots$ in the sector $\tfrac{1}{2}\pi < \theta < \tfrac{3}{2}\pi$. Since the sets $\{\cos[(2m-1)\theta]\}_{m=0}^{\infty}$ and $\{\cos(2m)\}_{m=0}^{\infty}$ are both complete in the interval $\tfrac{1}{2}\pi < \theta < \tfrac{3}{2}\pi$, it follows from (4.33a, b) that

$$b_{n,m} = \begin{cases} (4/\pi)\, m(m^2 - n^2)^{-1} & (n \text{ even, } m \text{ odd}), \\ (4/\pi)\, n(m^2 - n^2)^{-1} & (n \text{ odd, } m \text{ even}), \\ 0 & (n - m \text{ even}). \end{cases} \tag{4.34}$$

The only quantities that are left to determine are the a_n. If the double summation in (4.32) is interchanged, $\eta^{(1)}(r, \theta; T)$ can be expressed in the form

$$\eta^{(1)} = \sum_{m=0}^{\infty} \left\{ \sum_{n=0}^{\infty} a_n \Gamma_{nm}(r) \right\} \cos(m\theta), \tag{4.35a}$$

where $\qquad \Gamma_{nm}(r) = [\delta_{nm} Y_m(r) + b_{n,m} J_m(r)]/Y_n(a^{(0)})$,   (4.35$b$)

δ_{nm} being the Kronecker delta function between n and m. If we apply the boundary condition (4.31a) the a_n will be determined from the infinite set of linear equations

$$\sum_{n=1}^{\infty} a_n \Gamma_{nm}(a^{(0)}) = \mu^{-1} c_y^{(1)} a^{(0)} \delta_{m1},$$ (4.36)

with $m = 0, 1, 2, \ldots$. With the $b_{n,m}$ and a_n known the exterior solution is complete. The expression (4.36) implies that as the cold eddy is progressively ventilated the excited wave field will decrease in magnitude because $c_y^{(1)}(T) \to 0$ as $T \to \infty$.

As it turns out, relatively few a_n values need to be computed to be able to give a very accurate approximation to the infinite sums in (4.32) or (4.35). If we recall the fact that $Y_n(a^{(0)}) \to -\infty$ and $J_n(a^{(0)}) \to 0$ as $n \to \infty$ (Abramowitz & Stegun 1965), then clearly (4.34b) implies that $\Gamma_{n,m}(a^{(0)}) \approx \delta_{nm}$ for sufficiently large n or m. (This property motivated our normalization in (4.32a).) In practice, we found that for $n, m \gtrsim 12$ this property held. As a result, when it came to solving for the a_n from (4.36) very good results were obtained by approximating the infinite system with the leading 20×20 finite system of linear equations. (For all cases examined we found $|a_n| < 10^{-7}$ for $n > 15$.)

5. An example calculation for a parabolic eddy

In this section we shall illustrate the theory that we have developed with an example where the leading-order eddy has a simple parabolic shape. Throughout this section we shall adopt constant parameter values of $s = 5 \times 10^{-2}$, $\mu = 0.5$ and $\beta = 5 \times 10^{-3}$.

The $O(1)$ eddy configuration is given by

$$h^{(0)}(r; T) = \exp(-T)[1 - (r/a^{(0)})^2].$$ (5.1)

In figure 2(a) we plot a cross-shelf section (along $x = 0$) of the *total* eddy height $h^{(0)}(r; 0) + sy$ versus y for $-10 < y < 10$.

Substitution of (5.1) into (4.13a) can be evaluated analytically to yield

$$\eta^{(0)}(r; T) = \pi \exp(-T) \left\{ Y_0(r) \left[\left(\left(\frac{r}{a^{(0)}}\right)^2 - 1 \right) \tfrac{1}{2} r J_1(r) - \frac{r^2 J_2(c)}{(a^{(0)})^2} \right] \right.$$
$$\left. + J_0(r) \left[\left(1 - \left(\frac{r}{a^{(0)}}\right)^2 \right) \tfrac{1}{2} r Y_1(r) + \frac{r^2 Y_2(a^{(0)})}{(a^{(0)})^2} - Y_2(a^{(0)}) \right] \right\}, \quad (5.2)$$

for the region $r < a^{(0)}$. In figure 2(b) we plot a cross-shelf section (along $x = 0$) of $\eta^{(0)}(r; 0)$ versus y for $-10 < y < 10$.

As well, substitution of (5.1) into (4.13c) can be evaluated analytically to imply that the allowed set of eddy radii will satisfy

$$J_2(a^{(0)}) = 0,$$ (5.3a)

which, for convenience, we choose to rewrite in the form

$$a^{(0)} = j_{2,n},$$ (5.3b)

where $j_{2,n}$ is the nth (non-zero) zero of $J_2(*)$. Throughout this section we take the 'ground-state' radius $a^{(0)} = j_{2,1} \approx 5.136$.

Substitution of (5.2) into (4.29) implies that the time-dependent cross-shelf translation speed is given by

$$c_y^{(1)}(T) = 0.227 \exp(-T).$$ (5.3c)
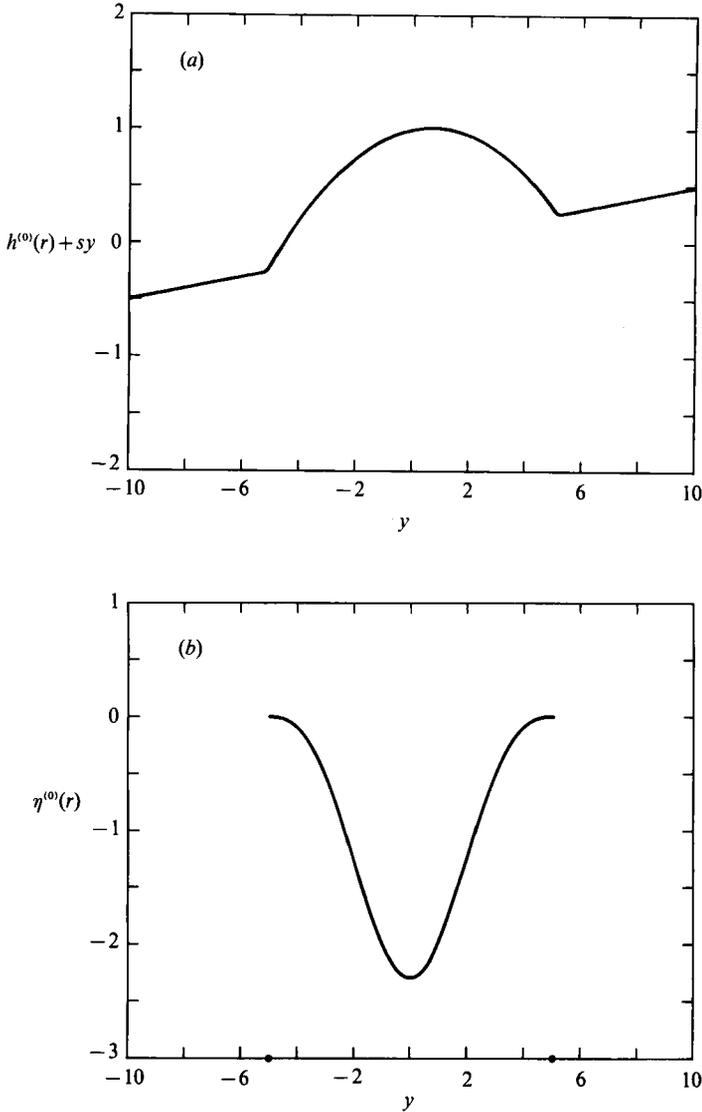
FIGURE 2. (a) A cross-shelf section of the parabolic eddy given by (5.1) on the sloping bottom at $T = 0$. (b) A cross-shelf section of the upper-layer $O(1)$ geostrophic pressure (immediately over the eddy depicted in (a) as determined by (5.2) at $T = 0$. The two dots on the y-axis denote the outer eddy boundary at $y = \pm a^{(0)}$.

We remark that the integral in the numerator of (4.29) was evaluated numerically. The *total* leading-order pressure in the eddy (see (3.15c)) is given by

$$p^{(0)}(r;T) = y + \mu(\eta^{(0)}(r;T) + h^{(0)}(r;T)), \tag{5.4}$$

where the first term corresponds to the dynamic pressure associated with gravity and the sloping bottom, and the remaining terms are responsible for generating the swirl velocity (i.e. the leading-order eddy azimuthal velocity relative to the leading-order along-shelf translation speed) in the eddy interior (see (4.15)). For convenience we shall denote the last two terms on the right-hand side of (5.4) as the 'swirl pressure'. Recall that the *Stern integral constraint* (4.14) will imply that the swirl pressure in the
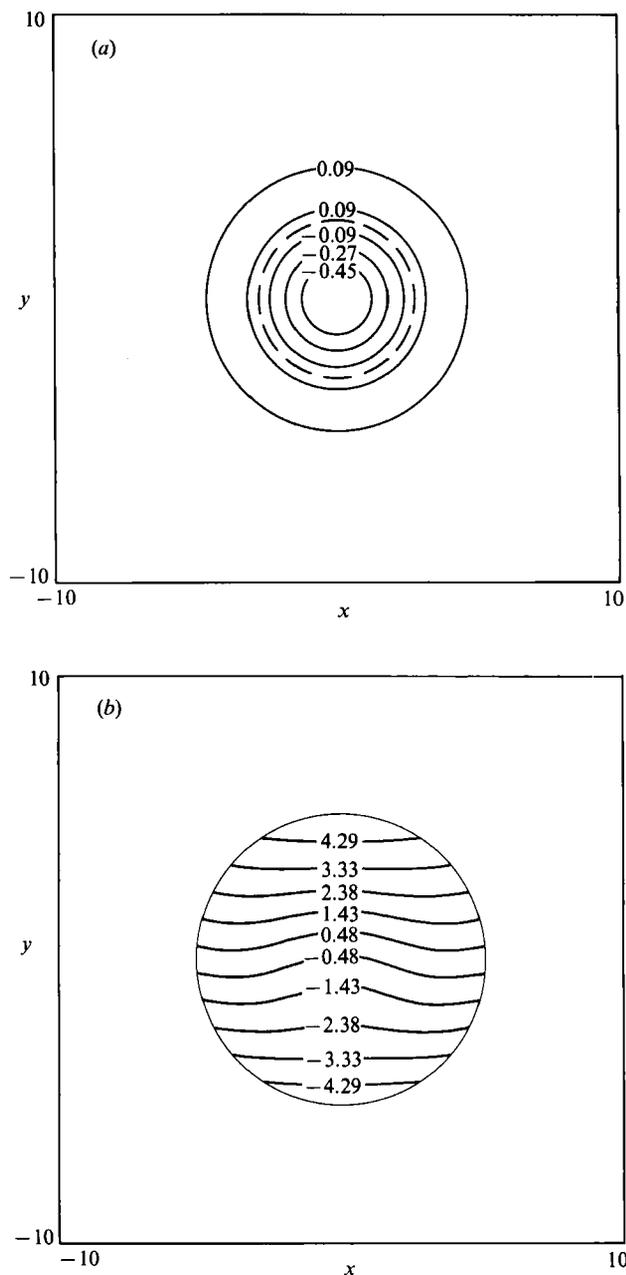
FIGURE 3. (a) A contour plot of the 'swirl' pressure $\mu[h^{(0)}(r;0)+\eta^{(0)}(r;0)]$ in the eddy. The dashed contour is the zero-value contour. Radially inward (outward) of the zero contour the swirl pressure anomaly is negative (positive) as demanded by the Stern integral constraint (4.14). (b) A contour plot of the *total* eddy geostrophic pressure field given by (5.4). The eddy geostrophic Eulerian velocity field is essentially the Nof speed (i.e. the along-shelf translation).

eddy must take on positive as well as negative values (if it is to be non-zero). In figure 3(a) we present a contour plot of the swirl pressure $\mu[h^{(0)}(r;0)+\eta^{(0)}(r;0)]$. The dashed contour is the 0-contour which occurs only once for the ground-state solution. The region of positive swirl pressure is located in $2.68 < r \leqslant a^{(0)}$. The region $0 < r < 2.68$
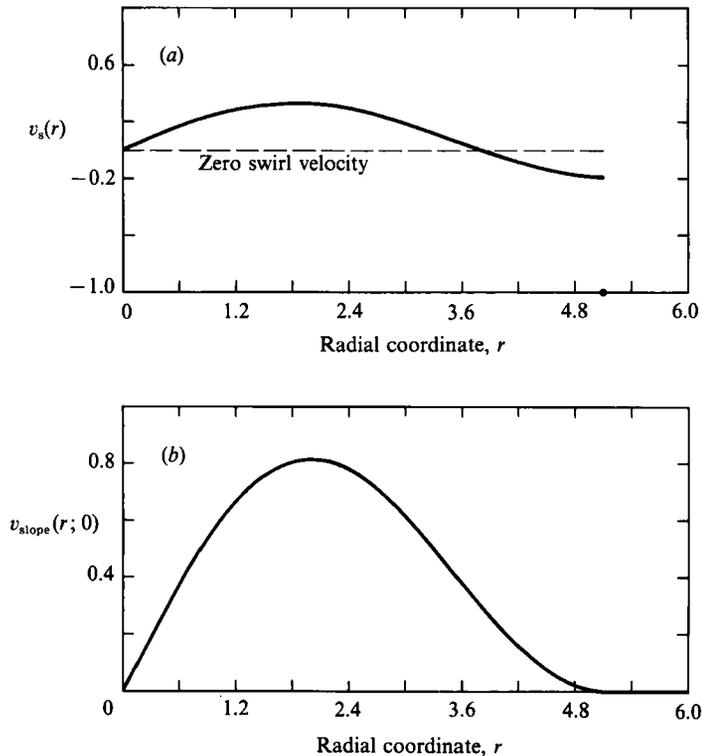
FIGURE 4. (a) The eddy swirl velocity as determined by (4.15). The velocities are non-dimensionalized with the Nof speed $g's/f \approx 2.5$ cm/s. The flow is mostly cyclonic with a small anticyclonic zone near the eddy boundary. The dashed horizontal line marks $v_s = 0$ and the dot on the r-axis denotes the eddy boundary $r = a^{(0)}$. (b) The cyclonic azimuthal velocity in the upper layer immediately over the eddy as determined by (5.5). The magnitude of the maximum dimensional azimuthal velocity is about twice as large as the maximum dimensional eddy swirl velocity.

has negative swirl pressure. The maximum swirl pressure is about 0.16 and occurs at $r \approx 3.83$. The minimum swirl pressure is located at $r = 0$ and has a value of approximately -0.65. These values scale linearly with the magnitude of the interaction parameter μ.

In figure 3(b) we present a contour plot of the total leading-order eddy pressure field $p^{(0)}(r;0)$ as given by (5.4). Because the magnitude of the swirl pressure is relatively small in comparison with the 'bottom slope' pressure contribution, the resulting contours are roughly speaking parallel to the isobaths. For realistic values of the interaction parameter (i.e. $\mu \approx 1$) there are no closed pressure contours. Consequently, to a stationary observer watching the cold-core eddy propagate, the relative velocity field in the eddy interior will appear almost negligible. This property has been observed in some rotating-tank experiments (J. A. Whitehead, personal communication). It is important to add, however, that the magnitude of the deflection in the pressure contours scales linearly with μ.

In figures 4(a) and 4(b) we present radial cross-sections of the leading-order swirl velocity and the azimuthal velocity in the upper layer, respectively, in the eddy region $r < a^{(0)}$ at $t = 0$. The eddy swirl velocity is given by (4.15) and the leading-order slope-water azimuthal velocity is given by

$$v_{\text{slope}}(r;T) = \eta_r^{(0)}(r;T). \tag{5.5}$$
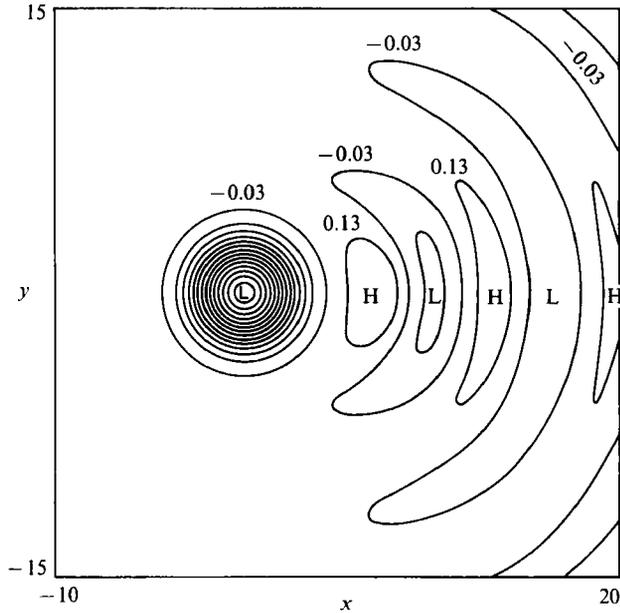
FIGURE 5. A contour plot of the complete leading-order geostrophic pressure field in the upper layer as determined by (5.6). The circular contours correspond to the strong cyclonic flow immediately over the eddy and the crescent-shaped contours correspond to the topographic Rossby wave field behind the propagating eddy. The H(L) symbols represent positive (negative) pressure anomalies and the contour interval is ± 0.16.

Recall that it followed from the Stern integral constraint (4.14) that the swirl velocity in the eddy must take on cyclonic *and* anticyclonic values. For our parabolic eddy model, there is a broad region $r \lesssim 3.85$; see figure 4(a) where the swirl velocity is cyclonic. The maximum magnitude of $v_s(r;0)$ in this cyclonic region is about 0.33. This would correspond to about $\frac{1}{3}$ of the Nof translation speed in dimensional units, or about 0.8–1.0 cm/s if the Nof speed is about 2.5–3.0 cm/s. Near the outer interior edge of the eddy $(3.8 \lesssim r < a^{(0)})$, the swirl velocity becomes anticyclonic. The maximum swirl velocity in this region for $T = 0$ is located along the eddy boundary and is about 20% of the Nof translation speed.

We can estimate the maximum slope-water azimuthal velocities from figure 4(b). The azimuthal slope-water velocity is cyclonic over the eddy region and has a maximum non-dimensional value of about 0.8 near $r = 2.0$. From (2.4) the scale velocity in the slope water is $\delta f L \approx 3.0$ cm/s which implies that the maximum *dimensional* azimuthal velocity in the slope water is about 2.5 cm/s. Hence if we compare the swirl velocity in the eddy interior (recall that this is defined to be the azimuthal velocity in the eddy interior relative to the along-shelf motion) to the slope water azimuthal velocity we see that the velocities in the slope water are on the order of twice the eddy swirl velocities.

In figure 5 we present a contour plot of the complete leading-order geostrophic pressure in the upper layer including the topographic wave field in $r > a^{(0)}$ for $T = 0$. That is, we have plotted $\eta(r, \theta; 0)$ as determined by

$$\eta(r, \theta; 0) = \begin{cases} \eta^{(0)}(r; 0) & \text{if } r < a^{(0)}, \\ \beta \eta^{(1)}(r, \theta; 0) & \text{if } r \geqslant a^{(0)}. \end{cases} \qquad \begin{array}{l} (5.6a) \\ (5.6b) \end{array}$$

Even though we have not included the $O(\beta)$ solutions in the eddy region $r < a^{(0)}$, we believe that by choosing β small enough (recall that $\beta = 5 \times 10^{-3}$), figure 5 is a correct asymptotic representation of the leading-order slope-water pressure field in $0 < r < \infty$. The circular contours in figure 5 correspond to the eddy-region (i.e. $r < a^{(0)} \eta^{(0)}(r; 0)$ solution and the remaining crescent-shaped contours correspond to the external (i.e. $r < a^{(0)}) \eta^{(0)}(r; 0)$ solution and the remaining crescent-shaped contours correspond to the external (i.e. $r > a^{(0)}) O(\beta)$ topographic wave field. The closed contours containing the H and L symbols correspond to regions of positive and negative pressure anomaly, respectively. The maximum wave amplitude occurs immediately behind the low-pressure region located over the eddy and has a magnitude of about 14 % of the minimum in the main low.

6. Summary and concluding remarks

A theory has been presented to describe the propagation of coherent cold-core baroclinic eddies on a sloping bottom and their dynamic and thermodynamic (i.e. ventilated) interaction with the surrounding ocean. The theoretical study presented in this paper was motivated by oceanographic observations (e.g. Ou & Houghton 1982; Houghton *et al.* 1982; Armi & D'Asaro 1980) and rotating-tank experiments (e.g. Mory 1983; Mory *et al.* 1987) on steadily travelling baroclinic eddies on a sloping bottom. Some of the properties of the oceanographic data, particularly the along-shelf translation speed, agreed with a theory proposed by Nof (1983) for these eddies. However, the data from the rotating-tank experiments did not seem to agree with the Nof theory.

Mory *et al.* (1987) suggested that frictional forces or dynamical interaction between the cold-core eddies and the surrounding slope water (neglected in the Nof theory) may be important. The possible importance of dynamical interactions is suggested by the *Stern integral constraint* (Mory 1983, 1985; see (4.14)) which requires that the area-integrated geostrophic pressure in the slope-water balance the area-integrated buoyancy force in the cold dome if the eddy–slope-water configuration is to be isolated. If this balance does not hold, then there will be an excited topographic wave field behind the propagating eddy (see Flierl 1984*a,b*) and a concomitant cross-shelf drift.

In the oceanographic context, other processes are also important. For example, the process of ventilation between the cold eddy and the relatively warmer slope water was of importance during the evolution of the cold dome described by Houghton *et al.* (1982) and Ou & Houghton (1982).

The new model equations (see (3.14) and (3.15)) developed in this paper to study the dynamical and ventilatory interactions between a cold-core eddy and the surrounding ocean on a sloping bottom corresponded to strongly interacting 'hybrid' quasi-geostrophic, intermediate-lengthscale geostrophic dynamics (see Charney & Flierl 1981). Based on parameter values suggested by the oceanographic data, the dynamics of the surrounding slope water is a quasi-geostrophic with relative vorticity induced by the vortex-tube compression associated with the passage of the ventilating cold-core eddy. The eddy dynamics is geostrophic but is *not* quasi-geostrophic because eddy height changes are not small in relation to the scale height of the eddy (see figure 1). The model equations were derived in a formal asymptotic expansion based on the shallow-water equations for a two-layer fluid assuming a small (appropriately scaled) shelf slope parameter.

Because of the discrete stratification used in our model, the parameterization we

adopted to describe the process of ventilation is the simple CI or cross-interfacial mass flux model of Dewar (1987, 1988a, b). This parameterization models the ventilation process as a continuous conversion of cold eddy water into relatively warmer slope water.

The model equations were solved using a multiple-scale asymptotic analysis valid in the limit of a relatively weak ventilation rate (but $O(1)$ dynamical interaction between the eddy and surrounding fluid) assuming an initially radially symmetric isolated eddy and slope-water configuration. The leading-order solution corresponds to a solitary baroclinic monopole configuration (see figure 2a, b) which propagates at the Nof speed and which satisfies the Stern integral constraint. For the simple parabolic eddy shape examined in §5, the swirl velocity in the eddy is about 30% of the Nof translation speed and about 50% of the Eulerian azimuthal velocity computed in the upper layer above the eddy. Consequently, to an external observer, the co-moving velocity field in the eddy would appear relatively quiescent in comparison to the slope-water velocity field above the eddy.

We are able to obtain an exact description of the induced topographic wave field behind the eddy (see figure 5) and to compute the associated cross-shelf translation velocity (see (4.29)). We find that the cross-shelf translation is positive (i.e. up the slope). If c_y^*, β^* and L denote the dimensional upslope speed, the dimensional ventilation rate (units of $1/s$), and the lengthscale, then $c_y^* \sim 0.227\beta^*L$ initially. The fact that $c_y^* > 0$ can be explained as a straightforward consequence of slope-water potential vorticity conservation and the ventilating eddy (see the discussion after (4.29)).

It has been suggested (Mory *et al.* 1987) that the eddies of the type studied in this paper may result from the baroclinic instability of pycnobathic or bottom gravity currents (see also Smith 1976; Shaw & Csanady 1983; Griffiths, Killworth & Stern 1982). The analysis by Griffiths *et al.* (1982) is restricted to long wavelengths and only contains a single layer. It is not difficult to show that (in the absence of diabatic processes) our two-layer model equations (3.14) and (3.15) admit exact along-shelf gravity current solutions. The stratification characteristics of these gravity currents will resemble a cold-core coupled density front on a sloping bottom. Swaters (1991) presents a detailed baroclinic instability analysis of these gravity current solutions.

Another interesting problem is the effect of bottom friction on the propagation characteristics of the isolated-cold-eddy solutions examined in this paper. Mory *et al.* (1987) suggested that frictional spin-down may be important in the dynamics, particularly in the rotating-tank simulations. It turns out that if one includes a simple Rayleigh damping term in the non-dimensional eddy momentum equations (2.5c) with an $O(1)$ dissipation coefficient, and subsequently examines a weak dissipation limit similar to the weak ventilation limit examined here (for the appropriately modifed (3.14), (3.15) and (3.16)), it can be shown that $h^{(0)}(r; T)$ must satisfy a fully nonlinear parabolic equation and that the along-shelf translation speed is smaller than the Nof speed. We are currently examining this problem and hope to be able to report on this in the future.

REFERENCES

ABRAMOWITZ, M. & STEGUN, I. A. 1965 *Handbook of Mathematical Functions*. Dover.

ARMI, L. & D'ASARO, E. 1980 Flow structures of the benthic ocean. *J. Geophys. Res.* **85** (C1), 469–483.

CHAPMAN, R. & NOF, D. 1988 The sinking of warm-core rings. *J. Phys. Oceanogr.* **18**, 565–583.

CHARNEY, J. G. & FLIERL, G. R. 1981 Oceanic analogues of large-scale atmospheric motions. In *Evolution of Physical Oceanography – Scientific Surveys in Honor of Henry Stommel* (ed. B. A. Warren & C. Wunsch), pp. 504–548. MIT Press.

DEWAR, W. K. 1987 Ventilating warm rings: theory and energetics. *J. Phys. Oceanogr.* **17**, 2219–2231.

DEWAR, W. K. 1988*a* Ventilating warm rings: structure and model evaluation. *J. Phys. Oceanogr.* **18**, 552–564.

DEWAR, W. K. 1988*b* Ventilating β-plane lenses. *J. Phys. Oceanogr.* **18**, 1193–1201.

FLIERL, G. R. 1984*a* Model of the structure and motion of a warm-core ring. *Austral. J. Mar. Freshw. Res.* **35**, 9–23.

FLIERL, G. R. 1984*b* Rossby wave radiation from a strongly nonlinear warm eddy. *J. Phys. Oceanogr.* **14**, 47–58.

GRIFFITHS, R. W., KILLWORTH, P. D. & STERN, M. E. 1982 Ageostrophic instability of ocean currents. *J. Fluid Mech.* **117**, 343–377.

HOUGHTON, R. W., SCHLITZ, R., BEARDSLEY, R. C., BUTMAN, B. & CHAMBERLIN, J. L. 1982 The middle Atlantic bight cool pool: evolution of the temperature structure during summer 1979. *J. Phys. Oceanogr.* **12**, 1019–1029.

KILWORTH, P. D. 1983 On the motion of isolated lenses on a β-plane. *J. Phys. Oceanogr.* **13**, 368–376.

McCARTNEY, M. S. 1975 Inertial Taylor columns on a beta plane. *J. Fluid Mech.* **68**, 71–95.

McKEE, W. W. 1971 Comments on 'A Rossby wake due to an island in an eastward current. *J. Phys. Oceanogr.* **1**, 287–289.

MILES, J. W. 1968 Lee waves in a stratified flow. Part 2. Semi-circular obstacle. *J. Fluid Mech.* **33**, 803–814.

MORY, M. 1983 Theory and experiment of isolated baroclinic vortices. *Tech. Rep.* WHOI-83-41, pp. 114–132. Woods Hole Oceanographic Institute.

MORY, M. 1985 Integral constraints on bottom and surface isolated eddies. *J. Phys. Oceanogr.* **15**, 1433–1438.

MORY, M., STERN, M. E. & GRIFFITHS, R. W. 1987 Coherent baroclinic eddies on a sloping bottom. *J. Fluid Mech.* **183**, 45–62.

NOF, D. 1983 The translation of isolated cold eddies on a sloping bottom. *Deep-Sea Res.* **30**, 171–182.

NOF, D. 1984 Oscillatory drift of deep cold eddies. *Deep-Sea Res.* **31**, 1395–1414.

OU, H. W. & HOUGHTON, R. 1982 A model of the summer progression of the cold-pool temperature in the middle Atlantic bight. *J. Phys. Oceanogr.* **12**, 1030–1036.

PEDLOSKY, J. 1987 *Geophysical Fluid Dynamics*, 2nd Edn. Springer.

SHAW, P. T. & CSANADY, G. T. 1983 Self-advection of density perturbations on a sloping continental shelf. *J. Phys. Oceanogr.* **13**, 769–782.

SMITH, P. C. 1976 Baroclinic instability in the Denmark strait overflow. *J. Phys. Oceanogr.* **6**, 355–371.

SWATERS, G. E. 1991 On the baroclinic instability of cold-core coupled density fronts on a sloping continental shelf. *J. Fluid Mech.* **224**, 361–382.

WHITEHEAD, J. A., STERN, M. E., FLIERL, G. R. & KLINGER, B. 1990 Experimental observations of a baroclinic eddy on a sloping bottom. *J. Geophys. Res.* **95**, 9585–9610.